Photopolymerizable composites based on vinyl acetate, p-acryloyloxybenzaldehyde and N-methacryloyloxyethyl-N'-fluoresceinyl urea as organic matrix for silver nanoparticles

V. E. PODASCA, T. BURUIANA, E. C. BURUIANA[*]
"Petru Poni" Institute of Macromolecular Chemistry, 41 A Grigore Ghica Voda Alley, 700487 Iasi, Romania

In the present paper, we report the generation of silver nanoparticles by *in situ* photoreduction of the silver salt into an organic matrix based on vinyl acetate (VAc), p-acryloyloxybenzaldehyde (AcrBzA), N-methacryloyloxyethyl-N'-fluoresceinyl urea (MA-Fl) and/or trietoxysilylpropyl carbamoyloxyethyl methacrylate (TCM) and phenyl-bis(2,4,6-trimethylbenzoyl) phosphine oxide (Irgacure 819) as photoinitiator. The formation of the nanoparticles (average diameter: 3-30 nm) in this manner has been confirmed using UV-vis, fluorescence and energy-dispersive X-ray (EDX) spectroscopy analysis, and transmission electron microscopy (TEM). The hybrid films emit fluorescence at 530 nm that could be quenched on the silver nanoparticles surface via electron and energy-transfer processes.

1. Introduction

Great interest has been focused on fabricating nanoparticle assemblies because they represent a popular route toward the preparation of advanced functional materials, and a modern concept in nanoscience and nanotechnology. [1] Polymer-nanoparticle (NP) composites may have various novel and improved properties originating from the synergism between organic and inorganic components. As a consequence, these nanocomposites have a large applicability in many important areas such as coatings, [2-4] inks, [5-8] dental materials [9], optical elements, [10, 11] photoresits, [12, 13], electron devices [14, 15], and so on.

One of common methods used for the obtaining of polymer/NPs composites involves a photochemical approach for the in situ synthesis of metal NPs and particularly, noble metals (silver, gold), created during the photopolymerization of some liquid monomers incorporating metal salt precursors [16]. The main feature of the photopolymerization process is that it occurs at room temperature and is typically rapid, allowing the system to overcome oxygen inhibition and moisture effect. In this direction, notable results have been performed by simultaneous photoinduced electron transfer and free-radical polymerization of the UV-curable acrylic formulations [17, 18]. For example, the hybrid materials including Ag or Au NPs were successfully utilized in nanomedicine, sensing, catalysis, nanoelectronics [19], and nanotechnology [20-23].

In order to exploit the unique properties of such materials it is needed that the stabilized nanostructures through host-guest interactions are uniformly distributed in the organic matrix, where the aggregation phenomenon has to be avoided. However, the control of the size and the shape of the NPs remains an important task from industrial and academic perspectives [24]. It can be said that the choice of the polymer is a key factor that affects the particles properties with a narrow size distribution and the final properties of nanohybrids intended for a specific application [25]. Hence, it is interesting to modify the structure of acrylic monomers including the urethane ones to promote the interaction of NPs with functional organic groups and produce improved dispersion of them in the polymer matrix [26, 27].

The objective of this research was obtaining hybrid polymer composites containing stable AgNPs prepared by reduction of silver nitrate through *in situ* way using UV light into a matrix based on vinyl acetate (VAc), p-acryloyloxybenzaldehyde (AcrBzA), N-metha-cryloyloxyethyl-N'-fluoresceinyl urea (MA-Fl) or trietoxysilylpropyl carbamoyloxyethyl methacrylate (TCM). The AgNPs have been characterized by transmission electron microscopy (TEM), UV-vis and energy-dispersive X-ray (EDX) spectroscopy analysis. Fluorescence properties of the films induced through fluorescein molecules covalently attached to the polymer backbone were also investigated.

2. Experimental part

Materials

Acryloyl chloride, p-hydroxybenzaldehyde, triethylamine, vinyl acetate (VAc), 1,1-azobis (cyclohexanecarbonitrile), fluoresceinamine isomer I, 2-isocyanatoethyl methacrylate, dibutyltin dilaurat, (3-isocyanatopropyl)triethoxysilane, 2-hydroxyethyl methacrylate, phenyl-bis(2,4,6-trimethylbenzoyl) phosphine oxide (Irgacure 819), silver nitrate ($AgNO_3$) were used as received (Aldrich).

Synthesis

AcrBzA and MA-Fl used in this study were synthesized according to the procedure reported in literature [28], while TCM was obtained in our laboratory. Then, the selected monomer mixtures were exposed to UV irradiation in the presence of Irgacure 819 as photoinitiator.

^{1}H NMR in DMSO-d_6 for poly(vinyl acetate-co-acryloyloxybenzaldehyde), (δ, ppm): 9.80 (aldehyde proton), 7.78 and 7.14 (aromatic protons in ortho and metha positions of benzaldehyde), 4.77 (methyne protons from ester), 1.99 (methyl proton from carbonyl neighboring groups), 1.95 (methyl protons), 1.92–1.77 (methylene protons).

Measurements

The structure of all synthesized derivatives was verified by FTIR, ^{1}H NMR, UV-vis and fluorescence spectroscopies. ^{1}H NMR and FTIR spectra were recorded on a Bruker 400 MHz spectrometer at room temperature, and on Bruker Vertex 70 instrument, respectively. The UV-vis absorption spectra were measured with a Specord 200 spectrophotometer in film state. The fluorescence intensity measurements were achieved with a Perkin-Elmer LS 55 equipment. The irradiations of the film containing silver salt were carried out using UV light with intensity of 50 mW/cm^2 generated by an Hg-Xe lamp (Hamamatsu Lightningcure Type LC58, Model L9588). Transmission electron microscopy (TEM) measurements were carried out at 100 kV using a Hitachi High-Tech HT7700 instrument. Microscopic investigations were performed on an environmental scanning electron microscope QUANTA200 coupled with an energy dispersive X-ray spectroscope (ESEM/EDX).

3. Results and discussion

Given the high reactivity of VAc in the radical polymerization, we began by examining the structure of copolymer obtained via photopolymerization of VAc with p-acryloyloxybenzaldehyde (formulation F1) under UV exposure. Indeed, in the NMR spectrum of the formed copolymer (data presented in experimental part) almost the same signals as those observed in poly(vinyl acetate-co-p-acryloyloxybenzaldehyde) synthesized by free radical polymerization appeared [28]. From the ^{1}H NMR analysis, it was appreciated that the binar copolymer derived from F1 is composed of 90 mol% VAc and only 10 mol% p-acryloyloxybenzaldehyde. Based on this result, other two formulations (F2, F3) differing by the presence of a fluorescent monomer (MA-Fl) or of hybrid methacrylate (TCM) in the mixture of VAc and AcrBzA were prepared and used in photopolymerization experiments. For comparison, we have prepared a formulation containing all the mentioned monomers (F4).

Our aim being the preparation of hybrid nanocomposites, 1 wt.% and 2.5 wt.% $AgNO_3$ were embedded inside each formulation, to form polymer-based composite films after UV irradiation. The molecular structure of monomers is shown in Scheme 1, and composition of the formulations is listed in Table 1.
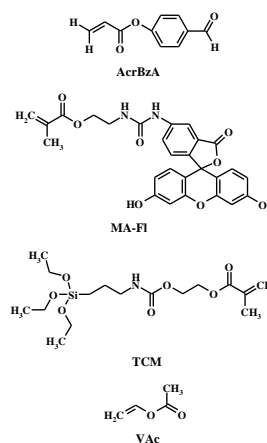
Scheme 1. Structure of AcrBzA, MA-Fl, and TCM monomers used in photopolymerization.

Table 1 Composition of the formulations and their degree of conversion.

Sample	AcrBzA (wt.%)	VAc (wt.%)	MA-Fl (wt.%)	TCM (wt.%)	Conv.[*] (%)
F1	20	80	-	-	97
F1+1% AgNO$_3$	20	80	-	-	92
F1+2.5% AgNO$_3$	20	80	-	-	87
F2	15	55	30	-	96
F2+1% AgNO$_3$	15	55	30	-	90
F2+2.5% AgNO$_3$	15	55	30	-	85
F3	25	50	-	25	95
F3+1% AgNO$_3$	25	50	-	25	88
F3+2.5% AgNO$_3$	25	50	-	25	82
F4	12.5	50	25	12.5	90
F4+1% AgNO$_3$	12.5	50	25	12.5	86
F4+2.5% AgNO$_3$	12.5	50	25	12.5	81

[*] conversion determined from FTIR

FTIR spectroscopy is largely used to follow the photopolymerization reaction that occurs in the case of acrylic derivatives. To study the photobehavior of the mono(meth)acrylates taken in combination with VAc, the disappearance of the characteristic acrylic double bond absorption at $1635\ cm^{-1}$ under UV irradiation was monitored. Fig. 1 presents the evolution of double bond for F1 versus irradiation time in the presence of 1.5 wt % Irgacure 819.

As can be seen, there are important changes in the infrared spectra of the monomers, where the polymerizable C=C stretching vibration at $1635\ cm^{-1}$ decreased gradually with increasing time of UV exposure. Under such conditions, the double bond conversion percentage for our formulations subsequently photopolymerized reached values between 90 and 97%, after 10 s of irradiation.

In the case of hybrid composites, the FTIR spectra of mixtures were very similar to those described, and in all formulations the values of the conversion degree were over 80%. This shows that the photopolymerization process is not significantly affected by the existence or absence of metal salt/Ag NPs.
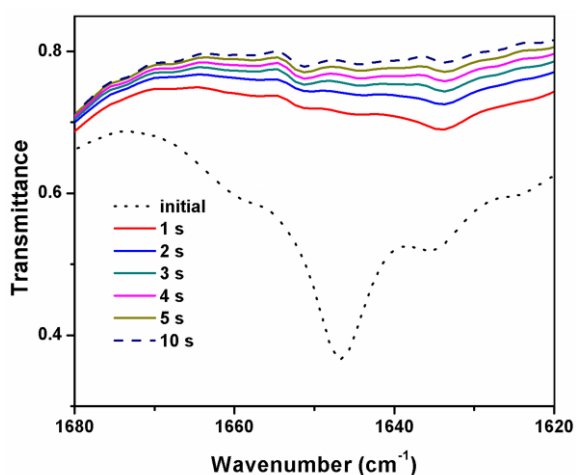

Fig. 1. Modification of the double bond for sample F1 monitored in the FTIR spectrum as a function of UV irradiation time.

Later on, reduction of the silver ions incorporated in the polymeric films was followed by measuring the UV–vis spectra. Fig. 2a displays the UV-vis spectra as a function of irradiation time, for the monomer mixture F1+1% $AgNO_3$. For closer observation, the kinetic course of generating AgNPs was evaluated at higher time intervals (905 s) of UV exposure of the above formulation. As result, an asymmetric surface plasmon absorption band located at 423 nm is observed. In the case of F2+2.5% $AgNO_3$ film (Fig. 2b) a bathochromic shift of the surface plasmon peak with about 30 nm was identified, photopolymerization process being much faster than in the other cases. Fig. 2c illustrates the plasmon absorption spectra at different irradiation times for all formulations with 1 wt.% $AgNO_3$. In fact, the plasmon absorption peaks

become visible between 401 and 451 nm, with a more intense band in F3+1% $AgNO_3$. It can be noted that in the formulations F3 and F4, the photopolymerization of the monomers is accompanied by the sol-gel reactions of the trietoxysilylpropyl carbamoyloxyethyl methacrylate. In Fig. 2d is presented the evolution of the UV-vis absorption spectra for F1, F2, F3, and F4 containing 2.5 wt.% $AgNO_3$ nanoparticles during UV irradiation. This behavior emphasizes the fact that the surface plasmon absorption peaks at about 420 nm (F1+2.5% $AgNO_3$), 405 nm (F3+2.5% $AgNO_3$) and at 450 nm (F4+2.5% $AgNO_3$) are originating from the nanosized character of the silver particles dispersed within the organic phase. It is well known that the surface plasmon resonance band appeared between 400 and 450 nm is a clear indicator of the formation of spherical silver particles [29].
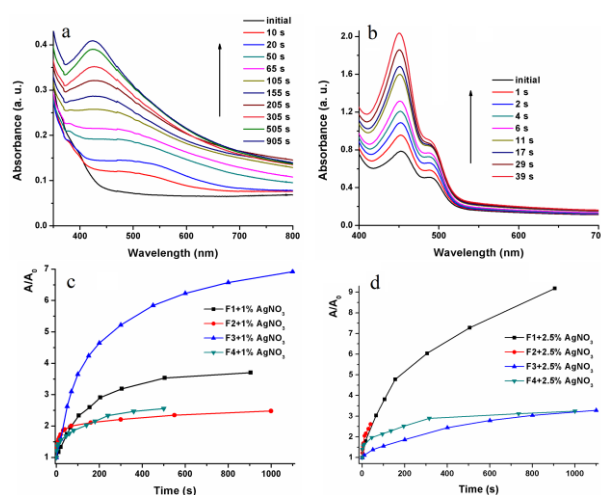

Fig. 2. The UV–vis spectra for F1+1% $AgNO_3$ (a), F2+2.5% $AgNO_3$ (b) and increase of the surface plasmon with irradiation time for 1% $AgNO_3$ (c) and 2.5% $AgNO_3$ (d).

In order to further understand the chemical composition of the photopolymerized films, EDX spectroscopy analysis was carried out using uniform thin films obtained by drop casting of monomer mixture and $AgNO_3$ on glass substrate. The EDX map of element presented in Fig. 3 shows the metallic silver particles on the surface of copolymer film resulted from F1+2.5% $AgNO_3$. Thus, silver atoms are displayed through the presence of bright spots which are uniformly distributed in the polymer matrix. The EDX elemental analysis of the hybrid films revealed the presence of carbon, oxygen, nitrogen, silicon and silver on the surface of these polymer composites (Table 2).

Sample	C (%)	O (%)	N (%)	Si (%)	Ag (%)
F1+1% AgNO$_3$	74.85	24.58	-	-	0.57
F1+2.5% AgNO$_3$	73.26	25.19	-	-	1.55
F2+1% AgNO$_3$	74.97	21.95	2.2	-	0.88
F2+2.5% AgNO$_3$	74.35	21.35	2.02	-	2.28
F3+1% AgNO$_3$	72.96	21.43	2.81	2.21	0.59
F3+2.5% AgNO$_3$	72.57	20.71	2.35	2.84	1.53
F4+1% AgNO$_3$	73.09	21.16	2.53	2.55	0.67
F4+2.5% AgNO$_3$	72.43	20.39	2.92	2.17	2.09
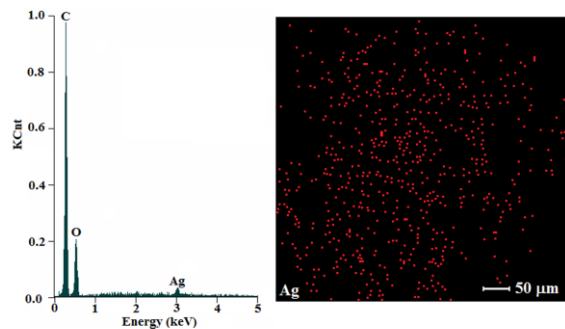
Fig. 3. EDX pattern, quantification data and corresponding EDX map collected from F1+2.5% AgNO$_3$ film.

Complementary, details of the morphology were performed using TEM analysis that allows a direct visualization of small silver particles. For the average diameter, approximately 100 particles were measured from digitized and magnified TEM image. The data on particle size were observed in the statistical size distribution given in Fig. 4. Therefore, F1+2.5% AgNO$_3$ film presents most of the particles in the 7–8 nm range (Fig. 4a), homogeneously distributed within the polymer matrix. For F2+2.5% AgNO$_3$ (Fig. 4b), the Ag NPs have a slight tendency of agglomeration, but most of them have average diameter between 3 and 10 nm. In the case of polymeric network based on F4+2.5% AgNO$_3$ (Fig. 4c, d), the resulting particles have sizes between 10 and 30 nm, and tend to agglomerate into clusters of about 200 nm.
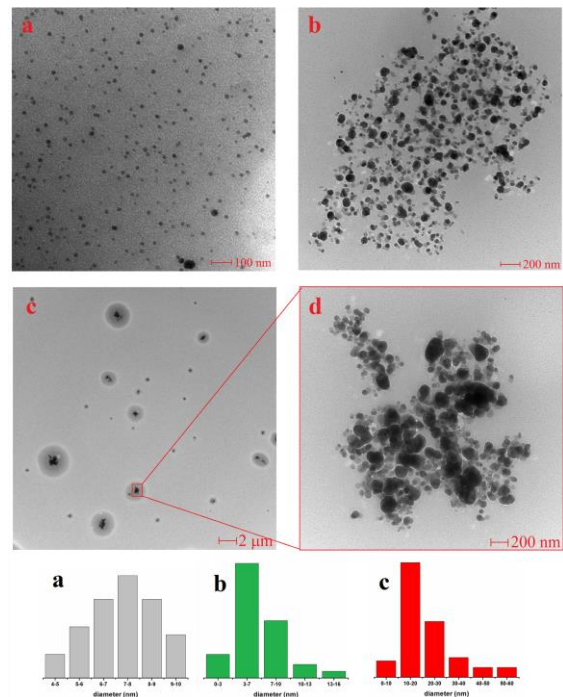
Fig. 4. TEM image and statistical size distribution of the silver nanoparticles dispersed into F1+2.5% AgNO$_3$ (a), F2+2.5% AgNO$_3$ (b), F4+2.5% AgNO$_3$ (c) and F4+2.5% AgNO$_3$ (d) enlargement of the square field in (c).

In addition, the fluorescence spectra of the formulations containing MA-Fl with and without Ag NPs (F2, F4) were recorded in the film state. In the fluorescence spectra (Fig. 5) there were changes in the fluorescence characteristics between the pure films and the corresponding hybrid composites. On excitation of the polymer films at 340 nm, these showed an emission band at around 531 nm (F2) and at 554 nm (F4) due to the fluorescein molecules present in the polymer structure. Upon the formation of Ag NPs, the fluorescence intensity decreased with increasing nanoparticles content. Thus, for F2+2.5% AgNO$_3$ film this decreased at 90.6%, whereas for F4+2.5% AgNO$_3$ the fluorescence intensity is reduced up to 45.6%.
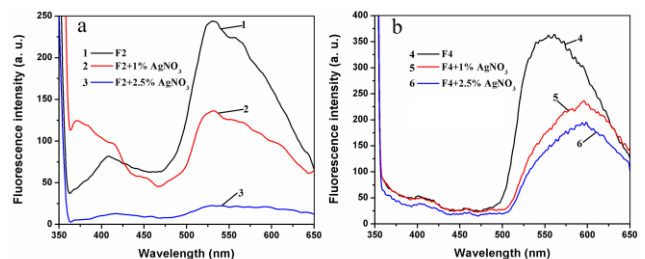

Fig. 5. Fluorescence emission spectra of F2 (a) and F4 (b) with and without nanoparticles.

It is thought that the access of a nanoparticle to fluorophore to achieve a fluorescence quenching by an electron and energy-transfer processes is slightly hindered into a matrix where there are siloxane (Si-O-Si) linkages formed via sol-gel process. Again, a bathochromic shift of 40 nm was observed in the later. Elucidating the detailed mechanism involved in the quenching of fluorescence in the proximity of the Ag NPs surface will be subject of a subsequent publication.

4. Conclusions

In summary, we prepared a series of hybrid nanocomposites using a photopolymerizable monomer mixture based on vinyl acetate, p-acryloyloxybenzaldehyde and N-methacryloyloxyethyl-N'-fluoresceinyl urea as fluorescent monomer, and 1 wt.% or 2.5 wt.% $AgNO_3$. In two formulations trietoxysilylpropyl carbamoyloxyethyl methacrylate was also incorporated in order to yield polymer networks. The synthesis of silver nanoparticles was achieved simultaneously with polymerization of the monomers exposed to UV irradiation, and their presence was confirmed by UV–Vis and EDX spectroscopy, and TEM analysis. Additionally, small silver NPs are efficient quenchers of molecular fluorescence, and therefore, such materials are promising for biological sensors and optoelectronic devices.

Acknowledgment

References

[1] Z. Tang, N. A. Kotov, Adv. Mater. **17**, 951 (2005).

[2] S. Zhou, L. Wu, B. You, G. Gu, Smart Coatings II, Acs Symposium Series, Ed. T. Provder, American Chemical Society, 2009, p. 193.

[3] K. Das, S. S. Ray, S. Chapple, J. Wesley-Smith, Ind. Eng. Chem. **52**, 6083 (2013).

[4] W. Sun, W. Sun, M. R. Kessler, N. Bowler, K. W. Dennis, R. W. McCallum, Q. Li, X. Tan, ACS Appl. Mater. Interfaces **5**, 1636 (2013).

[5] N. A. Harum, M. J. Benning, B. R. Horrocks, D. A. Fulton, Nanoscale **5**, 3817 (2013).

[6] W. K. Lee, Z. Dai, W. P. King, P. E. Sheehan, Nano Lett. **10**, 129 (2010).

[7] A. Chiolerio, V. Camarchia, R. Quaglia, M. Pirola, P. Pandolfi, C. F. Pirri, J. Alloys Comp. **615**, S501 (2014).

[8] M. Sangermano, A. Chiolerio, G. Marti, P. Martino, Macromol. Mater. Eng. **298**, 607 (2013).

[9] U. Lohbauer, Materials **3**, 76 (2010).

[10] A. Lopez-Santiago, H. R. Grant, P. Gangopadhyay, R. Voorakaranam, R. A. Norwood, N. Peyghambarian, Opt. Mat. Express **2**, 978 (2012).

[11] F. Cui, J. Zhang, T. Cui, S. Liang, B. Li, Q. Lin, B. Yang, Nano Res. **1**, 195 (2008).

[12] T. Hanemann, D. V. Szabo, Materials **3**, 3468 (2010).

[13] M. Lillemose, L. Gammelgaard, J. Richter, E. V. Thomson, A. Boisen, Comp. Sci. Tech. **68**, 1831 (2008).

[14] A. Chiolerio, M. Sangermano, Mater. Sci. Eng. B **177**, 373 (2012).

[15] A. Chiolerio, L. Vescovo, M. Sangermano, Macromol. Chem. Phys. **211**, 2008 (2010).

[16] W. D. Cook, Q. D. Nghiem, Q. Chen, F. Chen, M. Sangermano, Macromolecules **44,** 4065 (2011).

[17] M. Sangermano, Y. Yagci, G. Rizza, Chem. Commun. **24**, 2771 (2008).

[18] L. Balan, M. Jin, J. P. Malval, H. Chaumeil, A. Defoin, L. Vidal, Macromolecules **41**, 9359 (2008).

[19] A. Chiolerio, I. Roppoloa, M. Sangermano, RSC Adv. **3**, 3446 (2013).

[20] E. C. Buruiana, A. Chibac, T. Buruiana, V. Melinte, L. Balan, J. Nanopart. Res. **15**, 1335 (2013).

[21] J. M. Kohler, I. Kraus, J. Faerber, C. Serra, J. Mater. Sci. **48**, 2158 (2013).

[22] D. T. Nguyen, D. H. Kim, K. S. Kim, Micron **42**, 207 (2011).

[23] P. Zhao, N. Li, D. Astruc, Coord. Chem. Rev. **257**, 638 (2013).

[24] A. Chiolerio, M. Cotto, P. Pandolfi, P. Martino, V. Camarchia, M. Pirola, G. Ghione, Microelectronic Eng. **97**, 8 (2012).

[25] B. A. Rozenberg, R. Tenne, Prog. Polym. Sci. **33**, 40 (2008).

[26] A. Chibac, V. Melinte, T. Buruiana, L. Balan, E. C. Buruiana, Chem. Eng. J. **200-202**, 577 (2012).

[27] T. Buruiana, V. Melinte, F. Jitaru, E. C. Buruiana, L. Balan, J. Polym. Sci. Part A Polym. Chem. **50**, 874 (2012).

[28] E. C. Buruiana, V. E. Podasca, T. Buruiana, Designed Monomers and Polymers **17**, 89 (2014).

[29] Y. Sun, Y. Xia, Analyst **128**, 686 (2003).

_____
[*]Corresponding author: emilbur@icmpp.ro